Chapter 7

Postsynthesis Treatment Influence on Hydrogen Sorption Properties of Carbon Nanotubes

Michail Obolensky, Andrew Basteev, Vladimir Beletsky, Andrew Kravchenko, Yuri Petrusenko, Valeriy Borysenko, Sergey Lavrynenko, Oleg Kravchenko, Irina Suvorova, Vladimir Golovanevskiy and Leonid Bazyma

Additional information is available at the end of the chapter

http://dx.doi.org/10.5772/50151

1. Introduction

It has been shown in the previous investigations (Pradhan et al., 2002; Obolensky et al., 2011a, 2011b) that the postsynthesis treatment (e.g. chemical, heat treatment, milling, irradiation etc.) of single-walled carbon nanotubes (SWCNT) can essentially change their sorption properties. Methods of SWCNT synthesis and features of the postsynthesis treatment of the SWCNT show in numerous experiments a wide range of gas (e.g. hydrogen etc.) mass contents in SWCNT ranging from extremely low (less than 0.1 wt%) to significantly high (more than 6 wt%) values. Unfortunately, none of the claims of hydrogen storage exceeding the DOE limit have been confirmed. For recent review of effect of synthesis method and post-treatment of CNTs, see Ref. (Chang & Hui-Ming, 2005).

So, it is well established that hydrogen storage capacity of CNTs depends on many parameters including their pretreatment, types and structural modifications etc. One of the ways seems to be highly influential and it is the generation of appreciable structural defects in the tube walls. However, the increase in defects in graphitized layers of CNTs should be limited otherwise their structure would be destroyed which might lead to lowering of interaction or potential energy between the hydrogen molecules and carbon atoms. For instance, non-optimized electron irradiations severely destroy the graphitic network of CNTs (Banhart et al., 2002) which is not desirable for application purposes.

It has been reported that postsynthesis treatment can easily induce defects in the wall of SWCNT (Pradhan et al., 2002; Banhart et al., 2002; Hashimoto et al., 2004). The possibility of molecular hydrogen adsorption by the defect sites can also be considered. The experimental investigations of above mentioned factors as well as the result of irradiation on to SWCNT sorption capability are reported in this study.

2. Experimental

2.1. Materials

The arc-derived as-prepared (AP) SWNT material used in the present studies was obtained from Carbon Solutions, Inc.. All data reported here are collected using materials from the same batch of SWNT material.

The impurities in AP-SWNTs may be divided into two categories: carbonaceous (amorphous carbon and graphitic nanoparticles) and metallic (typically transition-metal catalysts). Thermogravimetric analysis (TGA) can be used to analyze the amount of metallic components quantitatively whereas Raman spectroscopy can be used to estimate qualitatively the carbonaceous impurities in AP and purified-SWNTs.

The AP SWNT (Carbon Solutions, Inc.) material has 21 to 31 percent of impurities which is consistent with the previously reported (Itkis et al., 2003) 34.5 ±1.8 percent impurities range. For purification of SWNTs the following technique has been used (Pradhan et al., 2002; Obolensky et al., 2011b). The SWNT (Carbon Solutions, approximately 1g amount) was oxidized in open air at 350^0C temperature for 30 minutes and then heated in 2.6 M HNO_3 for 20 hours. After above procedure the treated CNTs were flushed in methanol and then in water until the neutral reaction was achieved, dried in air and then were annealed in deep vacuum (10^{-8} bar) for 20 hours at 800^oC temperature. Identification of the gases allocated in an act of warming of a sample at 850^oC was carried by mass-spectrometry (MX-7203). Working pressure in the chamber of the mass-spectrometer was 10^{-4} Па. Approbation of nanotubes purify technology was carried out and 700 milligrams of the purified nanotubes were obtained (metal 6-9 at. %).

After chemical treatment, CNTs were milled at liquid nitrogen temperature in a stainless steel ball mill. Milling duration was 60 minutes with interruption after each 5 minutes for CNT samples' microscopic control. After the milling procedure finishing the "ball mill" was heated up to the room temperature and CNT samples were sieved through a 63 μm sieve (Obolensky et al., 2011b).

2.2. Experimental facility

The method for SWNT electron bombardment irradiation was elaborated. In contrast to (Obolensky et al., 2011a) where the exposure of γ – quantum 10^5 Rad was used (this dose is equal to regime of electron bombardment ~$3*10^{12}$ e^-/cm^2) the fluence in the work reported here was 10^{13}-$2*10^{15}e^-/cm^2$. The electron bombardment procedure was carried out at room temperature on the ELIAS linear accelerator (National Science Center "Kharkov Institute of Physics and Technology"). The electron energy was 2.3 MeV and beam intensity was 0.2 $\mu A/cm^2$. The main parameters of ELIAS accelerator are specified in Table 1.

Study of sorption/desorption process was carried out using the standard volumetric method (Obolensky et al., 2011a, 2011b). Hydrogen desorption out from SWNT was also

studied on the mass spectrometer MX7203. The schematics of the experimental facility used with both measurement methods is shown in Figure 1.

Parameters	Values
Energy of accelerated electrons	0.5- 3.0 MeV
Beam current (without scanning)	0.5-150 μA
Max beam current (with scanning):	up to 500 μA
Electron beam disperse	10^{-4} radian
Diameter of electron beam without focusing	1,0 cm
Diameter of electron beam with focusing, for 90% capacity	<1 mm
Vacuum in electron beam line	$1x10^{-7}$ mbar
Power consumption	20 κW

Table 1. Parameters of ELIAS accelerator

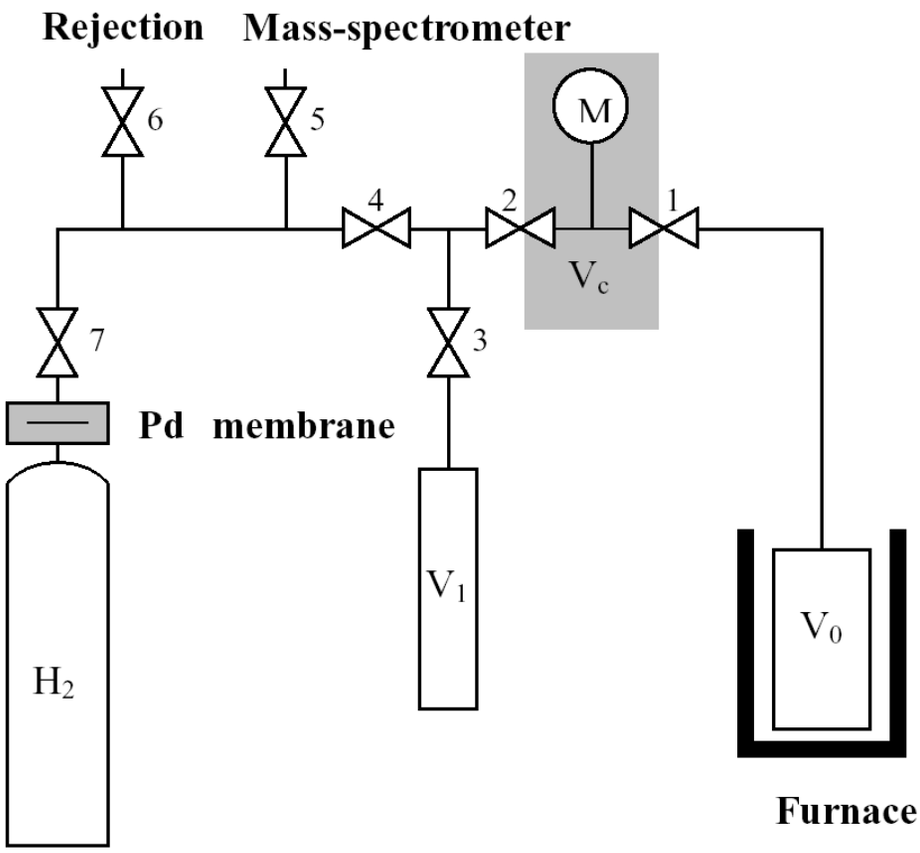

Figure 1. Experimental facility schematics (Obolensky et al., 2011b). Vc – total accurate including manometer and supply pipelines; V_1 – vessel with pure gas; V_0 – ampoule with carbon nanotubes sample; H_2 – non-purified hydrogen source

Raman spectra studies at ambient conditions with 514 nm laser line were carried out for some samples at the Physics Institute of the Penn State University.

3. Results

3.1. Adsorption studies of non-irradiated samples

Study of sorption/desorption process was carried out using the standard volumetric method on a custom designed and manufactured manufactured vacuum stainless steel facility which included the known good unit volume V_E and measuring vessel with volume V_M. Part of measuring vessel V_{78} was cooled down to liquid nitrogen vaporisation temperature of ~ 78 K. Before measurements the facility was calibrated. The good unit with volume V_E was inflated by gaseous helium or hydrogen with pressure P_I ~ 10 bar at room temperature which has been measured with ± 0.5 K precision. The pressure was controlled by electronic manometer GE Druck 104 with 1 mbar resolution. After the total facility volume V = VE + VM was filled up, the pressure dropped to the value of PF = VEPI(VE + VM - VA). This circumstance allowed exact determination of the volumes relation, taking into account the ampoule volume V_A without sample. Above relation for hydrogen and helium was found equal with approximately ~ 0.01 percent accuracy and therefore the hydrogen sorption by vacuum system elements could be excluded from consideration. After this procedure, the container with ampoule was cooled to temperature 78 K and relation P_W/P_F was determined, where P_W is the pressure in the system after cooling.

The measurement of physically absorbed hydrogen was conducted in accordance with the following procedure. Firstly, after cooling down the container to temperature 78 K the system was evacuated to pressure ~ 0.1mbar for gaseous hydrogen elimination. The next step was pressure increase registration in the system during container heating, caused by hydrogen desorption process.

The samples of SWNT with mass of 80 – 300 mg (estimated bulk density ~ 1000 kg/m^3) were used for the experiments on the volumetric facility. The pressure drop character dynamics during container with non-irradiated samples cooling are shown in Figure 2.

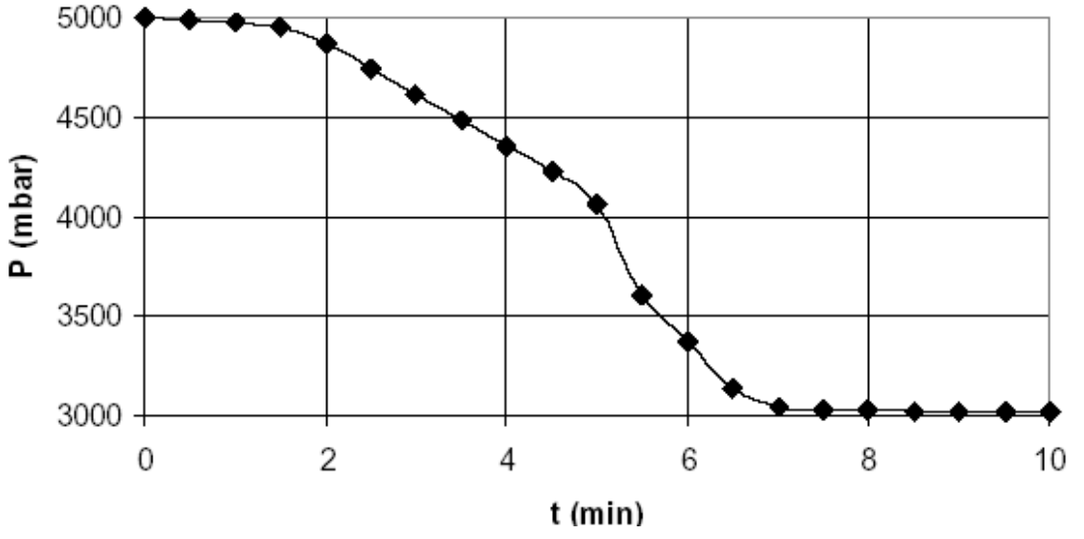

Figure 2. The dependence of pressure drop in the container with non-irradiated CNT samples upon time during container with samples cooling (P_F = 5035 mbar) (Obolensky et al., 2011b)

In Figure 2, one can see three sections with different sorption dynamics. On the base of comparison of this pressure drop dynamics with pressure drop dynamics for calibration stroke the following can be noted. The pressure drop relative to the empty container was observed already at room temperature during the letting-to-hydrogen and this pressure was noted at a ~ 20 mbar level. The additional pressure decrease was observed during further container cooling to 78 K temperature and at different cooling cycles this value was 10 – 15 mbar.

The pressure in the system during whole system heating was less than the pressure before the beginning of cooling by 10 – 12 mbar. Apparently this fact could be explained by any amount of hydrogen staying in binding state at room temperature after desorption. We didn't register this phenomenon on repeat of the heating-cooling cycles.

Figure 3 illustrates the correlation of pressure and temperature in the system for two evacuating regimes: fast (3 min) and gradual (15 min). Apparently already at 78 K temperature the increase of the duration of evacuation causes significant desorption and consequently elimination of part of hydrogen out from the system even before the beginning of heating. The duration of container heating for both regimes was approximately 25 – 30 min.

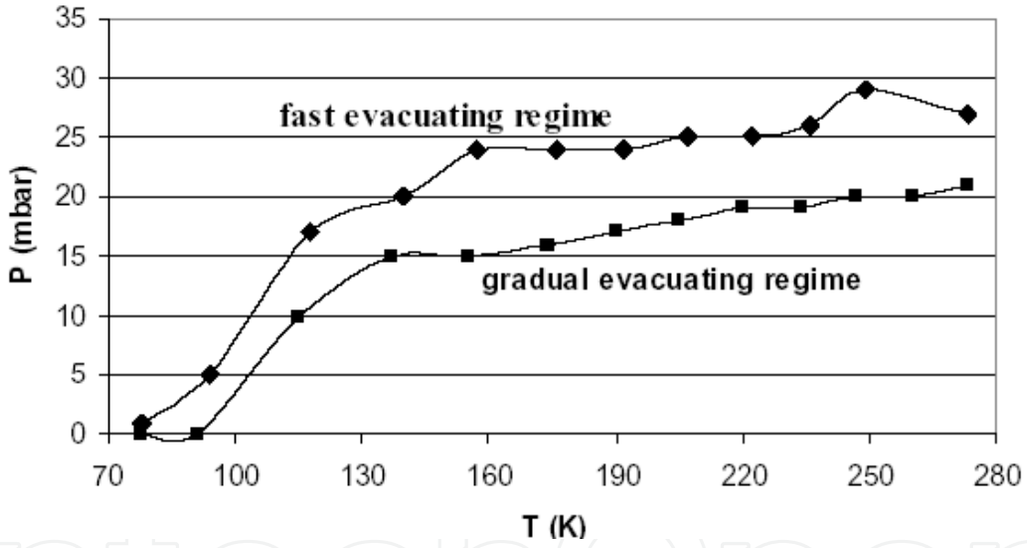

Figure 3. The dependence of pressure in the container with non-irradiated CNT samples upon temperature during container heating for different evacuation rates (Obolensky et al., 2011b)

The temperature dependences of hydrogen density in volume situated at heating regime (V_{78}) and in the rest facility volume at ambient temperature are shown in Figure 4. It could be seen that the main hydrogen mass is exuded at temperature T< 160 K that is caused by relatively low value of physical absorption activation energy. Pressure difference occurring at container heating without evacuating and initial pressure P_F as noted earlier is caused by other mechanism with higher values of desorption energies and it can be related to chemosorption regime with higher characteristic temperatures.

Our estimations show that at different sorption/desorption cycles the amount of hydrogen located in non-irradiated SWNT was equal to 0.12 ±0.2 mass percent.

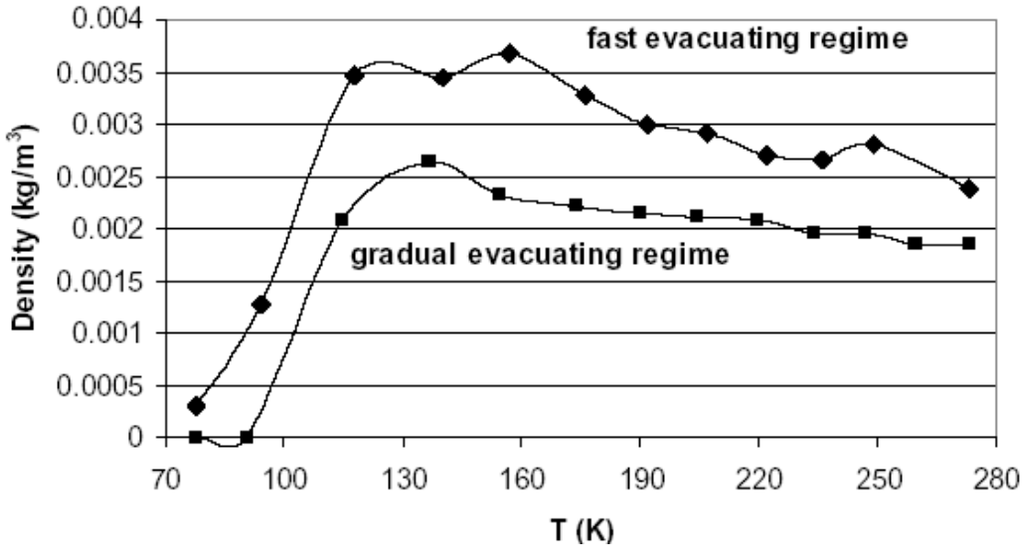

Figure 4. The dependence of hydrogen density in container with non-irradiated CNT samples upon temperature during container heating for different evacuation rates (Obolensky et al., 2011b)

3.2. Adsorption studies of irradiated samples

Hydrogen storage was studied with 2.5-90 mg samples. Saturation was carried out at liquid nitrogen temperatures (~78 K), and 300 K and at pressures between 3 and 10 bar. The measurement of physically absorbed hydrogen was conducted in accordance with the following procedure.

First, after cooling the container down to 78 K temperature the system was evacuated to ~ 0.1 mbar of pressure for gaseous hydrogen elimination. Next, pressure in the system during container heating up to room temperature caused by hydrogen desorption process was registered. Hydrogen desorption out from SWNT was also studied in the 0-900 C temperature range by mass-spectrometry method on the MX 7203 mass spectrometer.

Our estimations (Obolensky et al., 2011b) show that at different sorption/desorption cycles the amount of hydrogen located in non-irradiated SWNT was equal to 0.12 ±0.2 mass percent. Hydrogen desorption from treated and exposed to physical sorption/desorption procedure material at pressures ~3000 mbar as it is described above has been studied with the use of mass-spectrometry method within the 0 – 900 °C temperature interval on the MX 7203 mass spectrometer. The dependencies of the amount of hydrogen extracted from non-irradiated (a) and irradiated up to the fluence of 10^{14} e-/cm^2 (b) SWNT samples upon temperature are shown in arbitrary units in Figure 5.

As can be seen from Figure 5 the amount of hydrogen desorbed from irradiated material is approximately 2.5 times higher compared with that desorbed from the non-irradiated material. We have to draw attention to the fact that all procedures of the sorption/desorption processes were carried out at the 78 – 300 K temperature interval but at the same time significant amount of hydrogen is desorbed at temperatures higher than 300 K. There are additional peaks on the desorption curve which apparently correspond with different

sorption sites appearing as the result of irradiation and can be characterized by various activation energies. It should be noted that over a long period of time of samples staying in air between irradiation procedures and hydrogen saturation, complete saturation generated by irradiation sites filling by the molecules of other gases has not been detected. The data in Figure 5 can be presented in another form (Figure 6) i.e. as additional amount of hydrogen desorbed from irradiated sample (Δ - the difference between the irradiated and not irradiated samples).

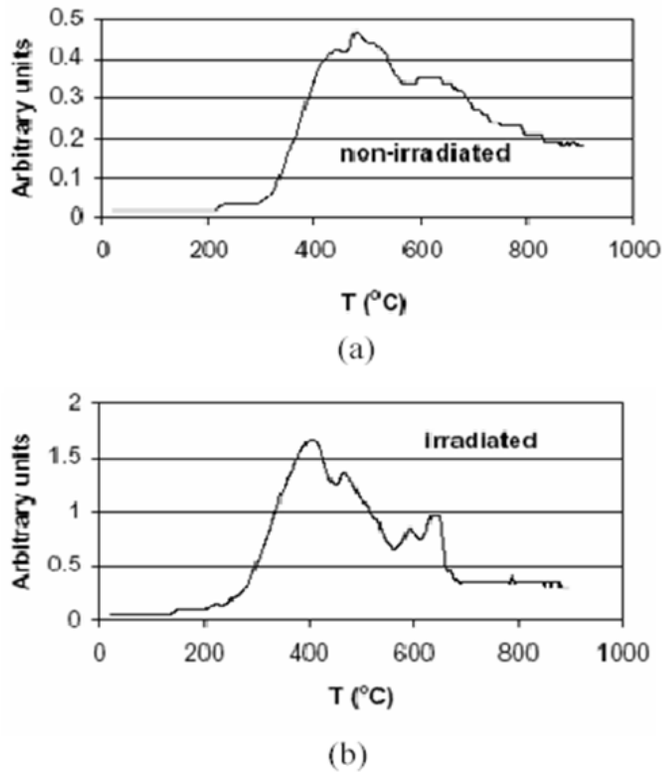

Figure 5. The dependencies of amount of hydrogen (arbitrary units) exuded from non-irradiated (a) and irradiated up to fluence 10^{14} e^-/cm^2 (b) samples upon temperature (Obolensky et al., 2011b)

In order to control the structural transformations of CNTs, it is important to clearly understand the defect generation mechanism and to realize the extent of defects and their influence on sorption properties of CNTs. Acid or alkali treatment does not routinely improve the hydrogen storage capacity of CNT samples. A suitable ball-milling treatment and activation process can open the caps of CNTs and produce more structural defects, and therefore may be beneficial in improving their hydrogen storage properties (Chang & Hui-Ming, 2005). In this connection we investigated the effect of electron irradiation on the hydrogen adsorption property of SWNTs without mechanical milling.

Five AP samples (cf., Table 2) have been annealed in vacuum during 10 hours at 800^0C temperature. The first sample (#1) was retained as the control sample. Sample #2 has remained for control and three samples (#3-5) were irradiated with various fluence ($5*10^{14}$, 10^{15} and $2*10^{15}e^-/cm^2$). After that, four samples (#2-5) were saturated at 10 bar pressure for 3 hours at 78 K temperature..

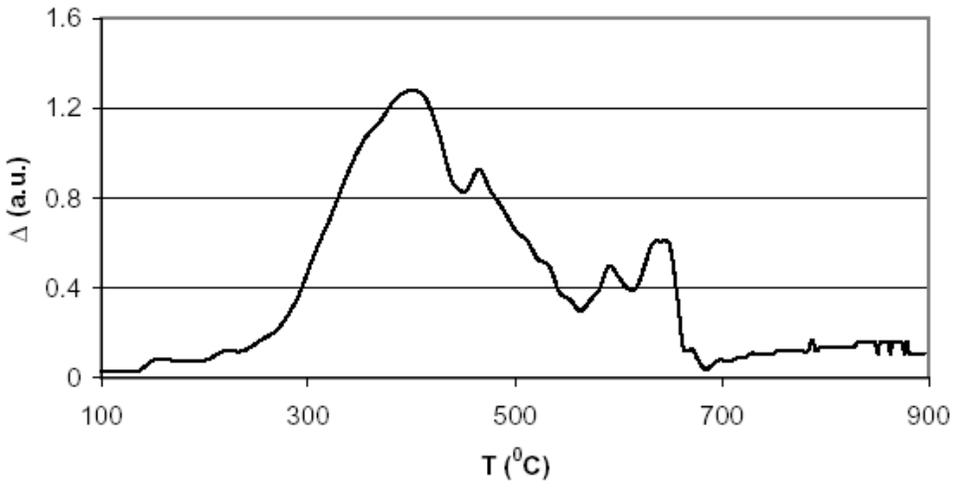

Figure 6. The dependence of additional amount of hydrogen (arbitrary units) desorbed from irradiated up to fluence 10^{14} e^-/cm^2 sample upon temperature (Obolensky et al., 2011b)

Sample	Vacuum anneal *T* (°C)/time (h)	Electron irradiation fluence (e^-/cm^2)/time (sec)	Hydrogen sorption *T* (K)/P (bar)	ΔH_2 (wt%)
1	800/10	-	-	-
2	800/10	-	~78/10	0.13
3	800/10	$5*10^{14}$/327	~78/10	0.12
4	800/10	10^{15}/706	~78/10	0.16
5	800/10	$2*10^{15}$/1340	~78/10	0.22

Note: For sample #2 ΔH_2 - the difference between irradiated and non-irradiated samples. For samples #3-5, ΔH_2 - thedifference between saturated and non-saturated samples.

Table 2. Sample history for adsorption studies

The dependencies of the amount of hydrogen extracted from the samples upon temperature are shown in arbitrary units in Figure 7. As can be seen from this Figure, the desorption curves were displaced in comparison with those for the samples exposed to all stages of treatment (i.e. oxidation, chemical treatment, annealing and milling shown in Figure 5..

For not irradiated samples the curves have remained similar, with some displacement of the maximum peak in the area of lower temperatures for the non-chemically treated and non-milled sample (2, Table 2). At the same time, the character of the curves for the irradiated samples (3-5, Table 2) essentially differs from the Ref. (Obolensky et al., 2011b). Characteristic peaks in the vicinity of 400 K and 650 K temperatures for the Ref. (Obolensky et al., 2011b) practically do not become visible for samples 3-5 (Table 2). With increase in fluence, the amount of hydrogen desorbed from irradiated samples is reduced for the given range of temperatures (Figure 8 and Figure 9).

As the temperature of samples at irradiation did not exceed 40^0C (Figure 10), most likely the temperature factor could not affect decrease in the amount of hydrogen desorbed from the irradiated samples in comparison with the non-irradiated samples. This feature needs additional study.

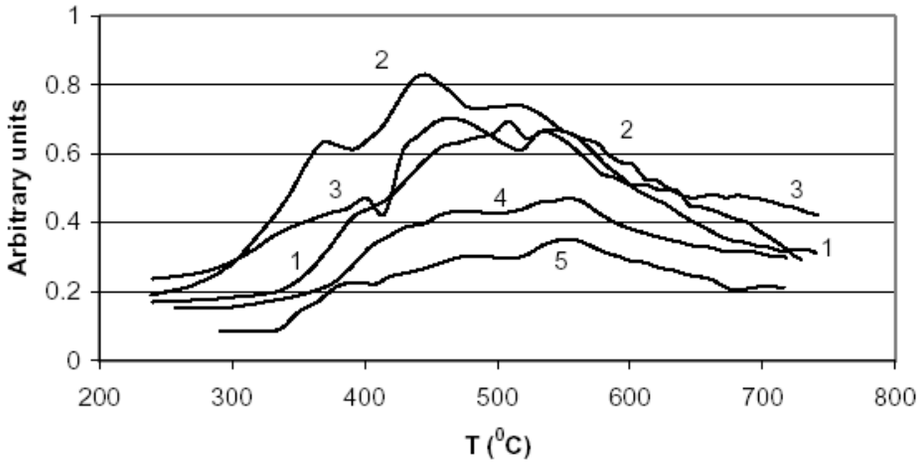

Figure 7. The dependencies of the amount of hydrogen (arbitrary units) exuded from samples (Table 1) upon temperature

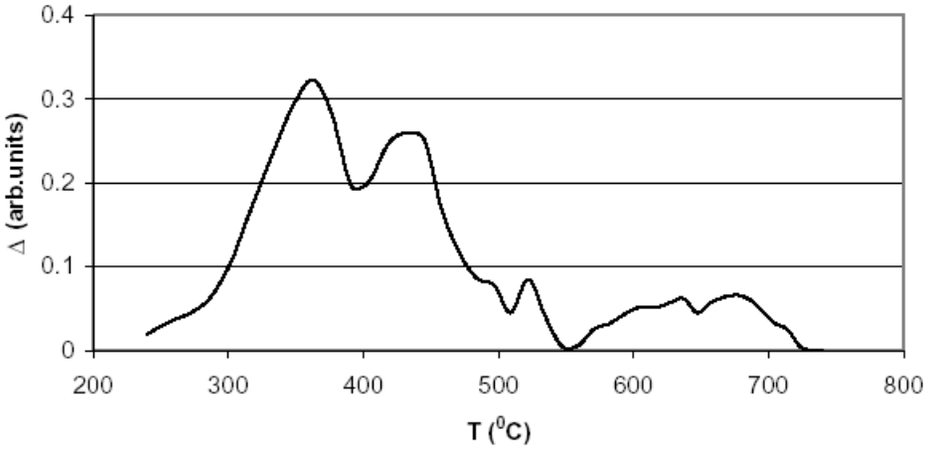

Figure 8. The dependence of the additional amount of hydrogen (the difference between saturated and non-saturated samples; arbitrary units) exuded from non-irradiated samples (Table 2) upon temperature

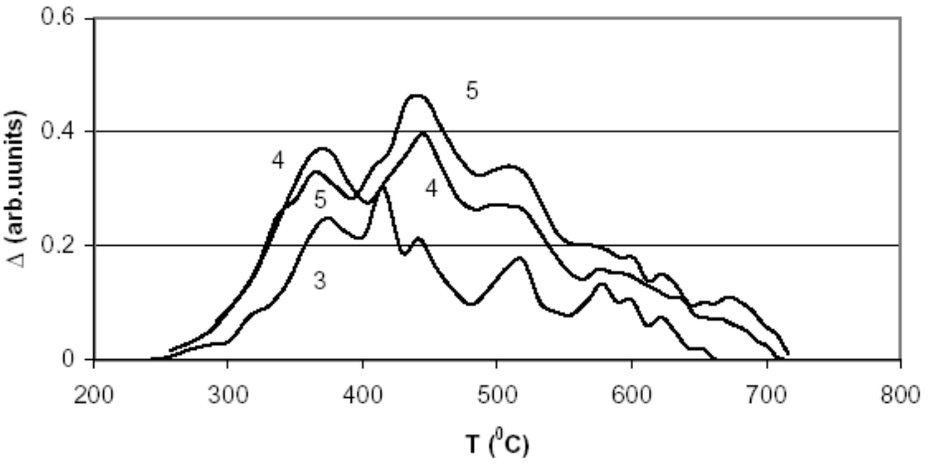

Figure 9. The dependencies of the additional amount of hydrogen (the difference between saturated non-irradiated sample and saturated irradiated samples; arbitrary units) for irradiated samples (Table 2) upon temperature

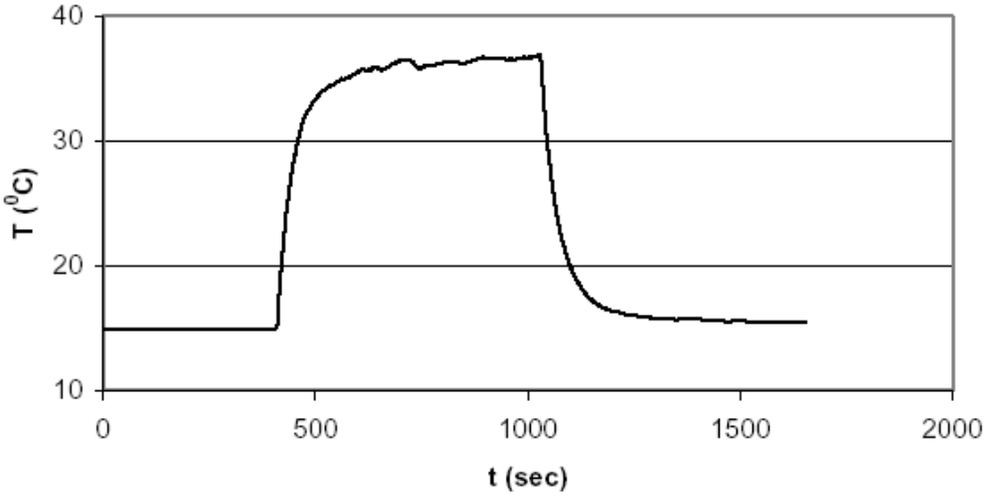

Figure 10. The dependence of samples temperature on the irradiation time (fluence $10^{15}e^{-}/cm^{2}$)

3.3. Raman scattering studies

Raman scattering is a sensitive probing of the structure and bonding in carbon materials, particularly carbon nanotubes. Raman scattering spectra for seven sets of samples (cf., Table 2) taken at room temperature in the range 100 to 3200 cm^{-1} are given in Figures 11-15..

The dominant spectral features include the low-frequency radial breathing modes (RBM) in the range approximately 150 to 200 cm^{-1} and the higher frequency modes in the range 1300 to 2700 cm^{-1} (Figure 11).

The SWNT tangential displacement modes observed near approximately 1600 cm^{-1} (G band) are related to the high frequency vibrational modes of a flat graphene sheet. The band (at 1300 cm^{-1}), commonly called the D band, has been observed in many sp^2-bonded carbon materials and is associated with disorder in the hexagonal carbon network.

Sample	Sample history	Vacuum anneal T (°C)/time (h)	Metal (at. %)
1	AP SWNTs [a)], irradiation [b)]	-	21-31
2	AP SWNTs [a)] irradiation [b)], sorption [c)]	-	21-31
3	AP SWNTs [a)], sorption [c)]	1000/20	21-31
4	Treated [d)], milling, sorption [c)]	1000/20	6-9
5	Treated [d)], milling, irradiation [b)]	-	6-9
6	Treated [d)], milling, irradiation [b)], sorption [c)]	-	6-9
7	Treated [d)], milling, irradiation [e)], sorption [c)]	1000/20	6-9

[a)] AP-SWNT "Carbon Solution"
[b)] Electron irradiation – 10^{13} e^{-}/cm^{2} (time – 375 sec)
[c)] Sorption – 78 K and 10 bar
[d)] Heated in 2.6 M HNO_3 during 20 hours
[e)] Electron irradiation – $2*10^{13}$ e^{-}/cm^{2} (time – 625 sec)

Table 3. Sample history for adsorption studies

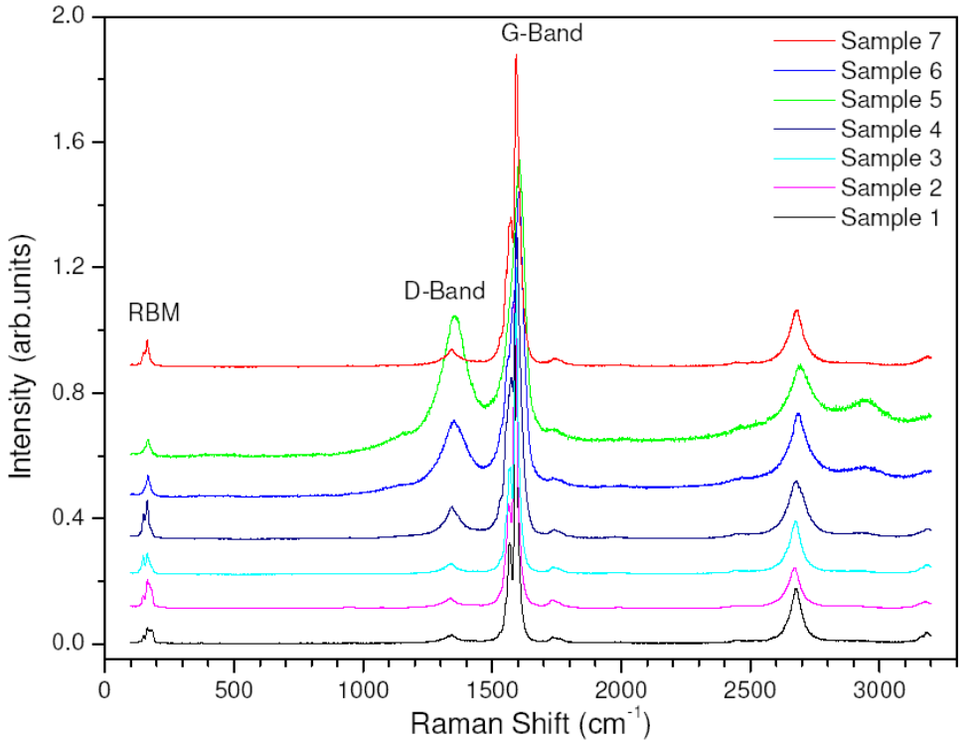

Figure 11. Room-temperature Raman spectra of bundles of arc-derived carbon nanotubes at various stages of post synthesis (Table 3). The Raman spectra were taken using 514-nm excitation

From the analysis of Raman spectra, it follows that the RBM frequency, ω_R, is inversely proportional to the tube diameter, d, while its value is up-shifted owing to the intertube interaction within a SWNT bundle (Pradhan et al., 2002). One of the empirical relations between d and ω_R, applicable for bundled SWNT is (Pradhan et al., 2002) is d (nm) = [224 cm^{-1} nm]/ [ω_R (cm^{-1}) - 12 cm^{-1}]. According to this equation, the main RBM peaks (Figure 12) at 163-166 cm^{-1} correspond to SWNT with a diameter of ~1.46 nm, whereas the shoulder at ~150 cm^{-1} is related to SWNT with a diameter of ~1.62 nm.

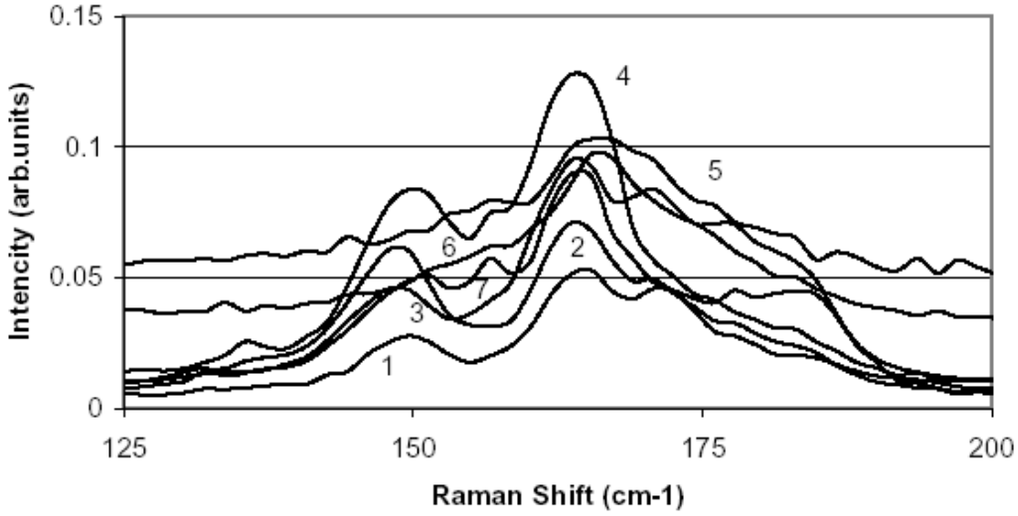

Figure 12. Raman spectra (RBM) at 514nm laser excitation energy (Table 3)

The intense Raman G-band at a higher energy corresponds to the C–C stretching vibrations in tangential and axial directions of the SWNT that splits to G^- (tangential) and G^+ (axial) bands located at 1566-1571 cm^{-1} and 1588-1602 cm^{-1}, respectively. The shape of the G^--band is sensitive to the electronic properties (strongly related to chirality) of SWNT.

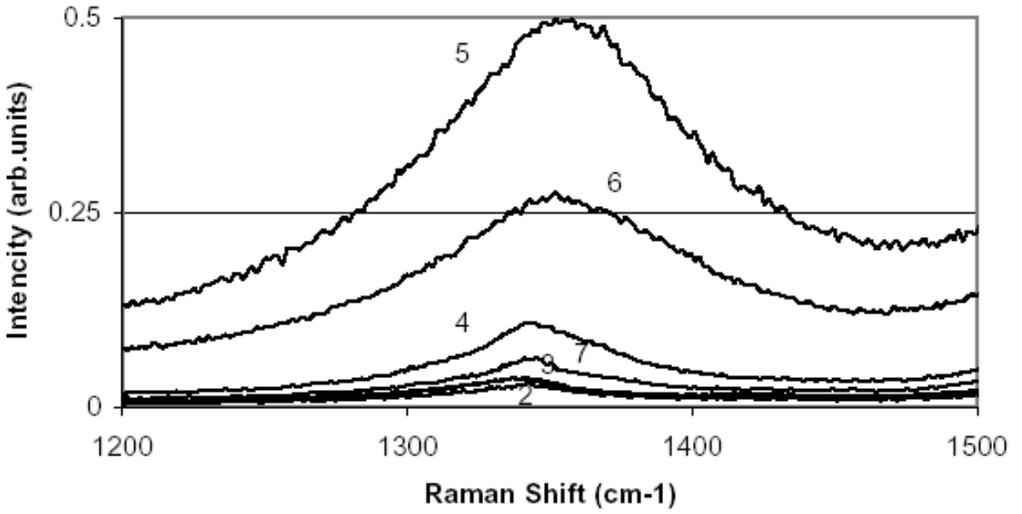

Figure 13. Raman spectra (D band) at 514nm laser excitation energy (Table 3)

D band (1341-1352 sm^{-1}, Figure 13) testifies to presence in samples of amorphous carbon and defects in structure of SWCNT. The ratio of peak intensity D band to peak intensity G band allows to judge as a level of crystallization and quantity of defects. It is possible to see that for samples which were not exposed to chemical treating and cryogenic milling (#1-3), intensity of peak D is minimal (0.03-0.036; I(D)/I(G)= 0.333-0.793, fig.14) and quantity of defects in structure of SWCNT was small.

Intensity of peak D band culminates for sample #5 (0.498; I(D)/I(G)= 2.129, Figure 14) which was exposed to chemical treating and cryogenic milling, but was not exposed to high-temperature heating in vacuum, to an irradiation and to hydrogen saturation.

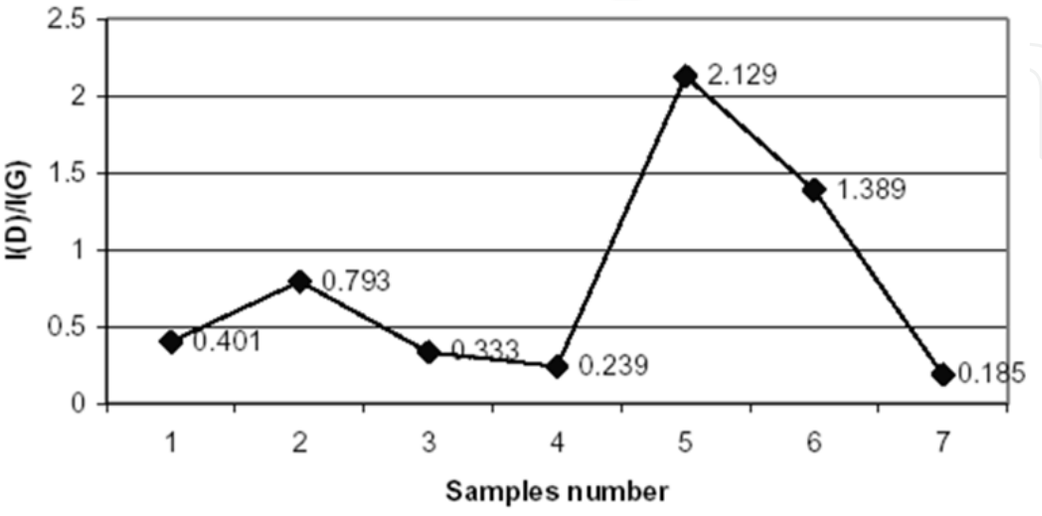

Figure 14. Distribution of the intensity ratio I(D)/I(G) for samples (Table 3)

Intensity of peak D for sample #6 which differed from sample #5 only on stages of hydrogen sorption is a little bit lower (0.275; I(D)/I(G)= 1.389, fig.14), but considerably exceeds intensity of peak D for samples #1-3. Apparently, during hydrogen sorption there was "treatment" of defects due to introduction of hydrogen in vacant sites of SWCNT.

Addition to the above-stated procedures of high-temperature heating in vacuum (samples #7 and #4) leads to essential decrease in intensity of peak D (0.062 and 0.107; I(D)/I(G)= 0.185 and 0.239, Figure 14). Most likely, at once two factors here dominate: treatment due to heating and treatment due to formation of C-H bond.

Range G' (2672-2686 cm^{-1}, Figure 15) which characterizes presence of "positive" or "negative" defects in SWCNT is submitted in spectra and has the obvious tendency: hydrogen sorption lowers intensity of this peak and leads to displacement of peak "to the left" in short-wave area of a spectrum.

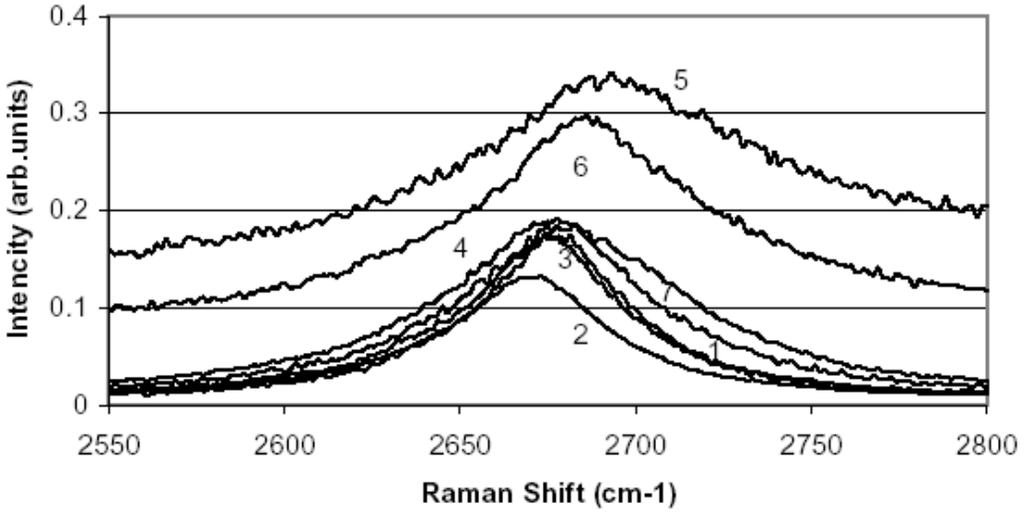

Figure 15. Raman spectra (G' band) at 514nm laser excitation energy (Table 3)

4. Conclusion

The amount of hydrogen desorbed from non-irradiated samples was 0.12 ±0.2 mass percent. The significant increase (more than two times) of hydrogen mass absorbed in irradiated SWCNT samples (10^{14} e^-/cm^2) relative to non-irradiated ones has been proved. For samples irradiated with fluences more than 10^{14} e^-/cm^2 the decrease of hydrogen desorption was observed.

Author details

Andrew Basteev and Leonid Bazyma
National Aerospace University "Kharkov Aviation Institute", Ukraine

Michail Obolensky, Andrew Kravchenko and Vladimir Beletsky
V.N. Karazin Kharkiv National University, Ukraine

Yuri Petrusenko, Valeriy Borysenko, Sergey Lavrynenko
National Science Center - Kharkov Institute of Physics and Technology, Ukraine

Oleg Kravchenko and Irina Suvorova
A.N. Podgorny Institute for Mechanical Engineering Problems, Ukraine

Vladimir Golovanevskiy
Western Australian School of Mines, Curtin University, Australia

Acknowledgement

This research was supported by Science and Technological Center in Ukraine, project #4957. The Raman measurements were performed at the Physics Institute of the Penn State University by Dr. Humberto R. Gutierrez and Dr. Xiaoming Liu.

5. References

Banhart, F.; Li J. X.; & Krasheninnikov, A.V. (2005) Carbon nanotubes under electron irradiation: stability of the tubes and their action as pipes for atom transport. *Phys. Rev.* B 71: 241408-4. ISSN 1098-0121.

Carbon Solutions, Inc.; web site: http://www.carbonsolution.com

Chang Liu, & Hui-Ming Cheng. (2005) Carbon nanotubes for clean energy applications. *J. Phys. D: Appl. Phys.* 38: R231–R252, ISSN 0022-3727

Itkis, M.E.; Perea, D.E.; Niyogi, S.; Rickard, S.M.; Hamon, M.A.; Hu, H.; Zhao, B. & Haddon R. C. (2003) Purity Evaluation of As-Prepared Single-Walled Carbon Nanotube Soot by Use of Solution-Phase Near-IR Spectroscopy. *Nano Lett.*, 3(3): 309-314, c.

Hashimoto, A.; Suenaga, K.; Gloter, A.; Urita, K.; & Iijima, S. (2004) Direct evidence for atomic defects in graphenelayers. *Nature* 430: 870-873, ISSN 0028-0836

Obolensky, M.A.; Basteev, A.V.; & Bazyma, L.A. (2011) Hydrogen storage in irradiated low dimensional structures. Fullerenes, *Nanotubes, and Carbon Nanostructures*, 19(1): 133-136, ISSN 1536-383X

Obolensky, M.; Kravchenko, A.; Beletsky, V.; Petrusenko, Yu.; Borysenko, V.; Lavrynenko, S.; Andrew Basteev, A. & Leonid Bazyma, L. (2011) Thermal, Chemical and Radiation Treatment Influence on Hydrogen Adsorption Capability in Single Wall Carbon Nanotubes. Fundamentals of Low-Dimensional Carbon Nanomaterials. Edited by John J. Boeck. *Mater. Res. Soc. Symp. Proc*. 1284: 125-130, ISBN 978-1-605-11261-9.

Pradhan, B.K.; Harutyunyan, A.R.; Stojkovic, D.; Grossman, J.C.; Zhang, P.; Cole, M.W.; Crespi, V.; Goto, H.; Fujiwara, J. & Eklund, P.C., (2002) Large cryogenic storage of hydrogen in carbon nanotubes at low pressures. *J. Mater. Res.* 17(9): 2209-2016, ISSN 0884-2914.